

**OPEN ACCESS**

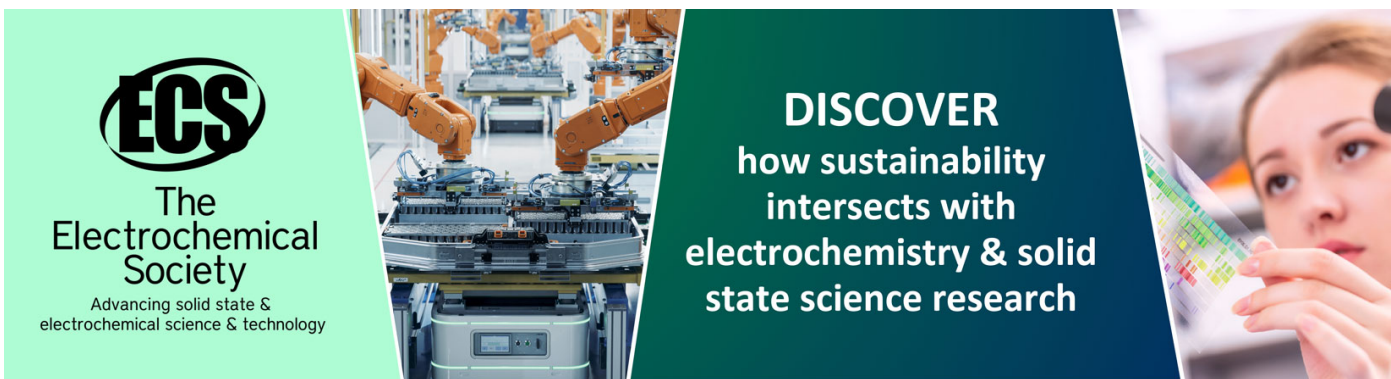
## Lattice defect assisted incorporation of $Mn^{2+}$ ions in cubic II-VI semiconductor quantum dots

To cite this article: S V Nistor *et al* 2010 *IOP Conf. Ser.: Mater. Sci. Eng.* **15** 012024

View the [article online](#) for updates and enhancements.

### You may also like

- [Taming excitons in II-VI semiconductor nanowires and nanobelts](#)  
Xinlong Xu, Qing Zhang, Jun Zhang et al.
- [Temperature Dependence of ZnS Growth with Atmospheric-Pressure Metalorganic Vapor Phase Epitaxy Using Ditertiarybutyl Sulfide](#)  
Toshio Obinata Toshio Obinata, Katsuhiro Uesugi Katsuhiro Uesugi, Go Sato Go Sato et al.
- [Mechanical and Vibrational Properties of ZnS with Wurtzite Structure: A First-Principles Study](#)  
You Yu, , Chun-Lin Chen et al.



**ECS**  
The  
Electrochemical  
Society  
Advancing solid state &  
electrochemical science & technology

**DISCOVER**  
how sustainability  
intersects with  
electrochemistry & solid  
state science research

# Lattice defect assisted incorporation of $\text{Mn}^{2+}$ ions in cubic II-VI semiconductor quantum dots

S V Nistor, M Stefan, L C Nistor, D. Ghica, C D Mateescu, J N Barascu

National Institute of Materials Physics, Atomistilor 105 bis, 077125 Magurele-Bucharest, Romania

E-mail: snistor@infim.ro

**Abstract.** Electron paramagnetic resonance spectra from substitutional  $\text{Mn}^{2+}$  ions in quantum dots of cubic ZnS with tight size distribution centred at 2 nm were recorded in the 9.8 GHz and 34 GHz frequency bands. Their quantitative analysis with line shape simulation and fitting computer programs accounting for both forbidden transitions and line broadening effects demonstrate the presence of a local axial distortion attributed to a neighbouring extended planar stacking defect. The presence of such extended lattice defects, confirmed from a high resolution transmission electron microscopy study on presently investigated cubic ZnS quantum dots, seems to be essential in the incorporation and localization of  $\text{Mn}^{2+}$  activating ions in other cubic II-VI semiconductor quantum dots as well.

## 1. Introduction

Activating impurities, in particular transition ions, are essential in fulfilling the expected exceptional properties of semiconducting nanocrystals. To understand the mechanisms responsible for their incorporation and to explain their local quantum properties, one needs to know the precise location of the doping impurities in the nanocrystals (NCs) lattice. In the case of wide band-gap nanocrystalline II-VI semiconductors, prepared at relatively low temperatures ( $< 350$  °C), such information could also help in understanding the still unclear mechanisms responsible for the incorporation of isoelectronic impurity ions such as  $\text{Mn}^{2+}$  or  $\text{Co}^{2+}$  [1,2].

Electron paramagnetic resonance (EPR) can accurately determine the localization of the paramagnetic impurities and the resulting changes in the neighbouring ligands configuration [3]. In the case of luminescent cubic ZnS (cZnS) NCs [4], it was generally accepted [1,5-10] that substitutional  $\text{Mn}^{2+}$  ions are arbitrarily localized at the cation ( $\text{Zn}^{2+}$ ) sites with local tetrahedral ( $T_d$ ) symmetry, as in the case of cZnS single crystals [11]. Despite this assumption, in the publications dedicated to this subject [6-10] the spin Hamiltonian (SH) describing the EPR spectra also included, besides the cubic Zeeman and hyperfine interaction terms with parameter values centred around  $g = 2.002$  and  $|A| = 64 \times 10^{-4} \text{ cm}^{-1}$  [11], axial and even rhombic zero-field-splitting (ZFS) terms characterized by the  $D$  and  $E$  parameters, respectively. Their reported values were spread over a two orders of magnitude range [6-10], a situation which can be explained by the low accuracy of the procedures used to determine the SH parameters. Moreover, no clear explanation for the presence of the non-cubic ZFS terms was given.

We have recently been able to obtain, by a surfactant-assisted liquid-liquid reaction at room temperature (RT), small cZnS NCs doped with Mn<sup>2+</sup> self-assembled into a mesoporous structure with a tight size distribution centred around 2 nm and an improved lattice quality, which was reflected in the EPR spectra with the smallest line-width reported so-far and a corresponding increase in resolution [12,13].

As will be further shown here, the full quantitative analysis of the resulting low and high frequency EPR spectra resulted in accurate SH parameters for the substitutional, as well as for the surface Mn<sup>2+</sup> centres. Our analysis confirms in the case of the substitutional centre the presence of an axial ZFS term, with an accurate finite  $D$  parameter value. Based on a comparison with early experimental data in strongly defective ZnS single crystal hosts, we demonstrate that the local axial crystal field component at the substitutional Mn<sup>2+</sup> ion is due to the presence of a neighbouring extended lattice defect (ELD), as a stacking fault or twin. We demonstrate that the ELDs play an essential role in the incorporation and localization of Mn<sup>2+</sup> ions in the cubic ZnS NCs lattice. Based on the similarity of the EPR spectra it is proposed that a similar extended lattice defects assisted (ELDA) mechanism of impurities incorporation is acting in the case of other cubic II-VI semiconductor NCs doped with Mn<sup>2+</sup> ions as well.

## 2. Experimental

The EPR investigations were performed on QDs of cZnS doped with 0.2% mol Mn<sup>2+</sup>, self-assembled into a mesoporous structure, which were prepared at RT by a surfactant-assisted liquid-liquid reaction [12]. The preparation procedure, as well as the results of structural and preliminary X-band EPR and optical characterization of the presently investigated sample batch were reported elsewhere [13,14]. The actual X(9.8 GHz)- and Q(34 GHz)-band measurements were performed at RT on EMX-plus and ELEXSYS 500Q spectrometers from Bruker, respectively. The SH parameters were determined by lineshape simulations and fitting procedures with the SIM specialized program graciously provided by Prof. H. Weihe of the University of Copenhagen and the EPRNMR v.6.4 program (Department of Chemistry, University of Saskatchewan, Canada).

## 3. Results and discussion

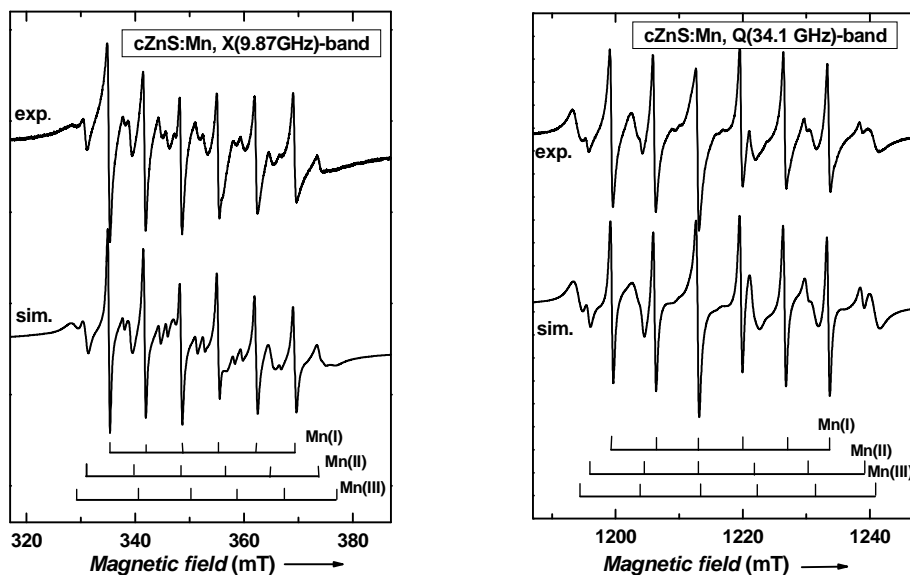
Our previous X-band EPR investigations of the cZnS:Mn QDs sample revealed the presence of a substitutional Mn<sup>2+</sup> centre, called Mn<sup>2+</sup>(I), which does not change its concentration by thermal treatments, and of two surface centres, called Mn<sup>2+</sup>(II) and Mn<sup>2+</sup>(III) [13]. The Mn<sup>2+</sup>(III) centres were found to transform into Mn<sup>2+</sup>(II) centres during heating, by a temperature activated desorption of water molecules from the nanocrystals surface [14].

Figure 1 (upper curves) presents the X- and Q – band EPR spectra of the mesoporous cZnS:Mn QDs sample. The transition fields attributed to the Mn<sup>2+</sup>(I), Mn<sup>2+</sup>(II) and Mn<sup>2+</sup>(III) centres are marked with vertical lines, namely 6 allowed ( $M_s: -1/2 \leftrightarrow 1/2, \Delta M_I = 0$ ) and 10 forbidden ( $M_s: -1/2 \leftrightarrow 1/2, \Delta M_I = \pm 1$ ) hyperfine transitions for the Mn<sup>2+</sup>(I) centres and only the 6 allowed hyperfine transitions for the Mn<sup>2+</sup>(II) and Mn<sup>2+</sup>(III) centres. These are well known features of the Mn<sup>2+</sup> ions in crystalline powders [3,15]. One should also mention that the forbidden transitions of the Mn<sup>2+</sup>(I) centres are visible only in the X-band. At the higher Q-band frequencies they are practically unobservable, the intensity ratio of the forbidden vs. allowed hyperfine transitions  $I_f/I_a$  being proportional [3] to  $(D/B)^2$ . The EPR spectra of the Mn<sup>2+</sup> centres in nanocrystalline cZnS are described by the following SH, with usual notations [3]:

$$H = \mu_B \vec{S} \hat{g} \vec{B} + \vec{S} \hat{A} \vec{I} + CF$$

Here the first two terms represent the main interactions of the  $S = 5/2$  electron spin with the external magnetic field and the hyperfine interaction with the  $I = 5/2$  nuclear spin of the <sup>55</sup>Mn (100% abundance) isotope, respectively. The last zero field splitting (ZFS) term describes the interaction of the electron spin with the local crystal field. In the case of a local cubic symmetry, similar to the pure

cubic ZnS single crystals lattice, the  $ZFS$  term is characterized by the  $a$  parameter, while for lower symmetry additional axial and rhombic terms are added, characterized by the  $D$  and  $E$  parameters, respectively [3].



**Figure 1.** Experimental (upper curves) and simulated (lower curves) X- and Q- band EPR spectra of mesoporous cZnS:Mn QDs. The simulated spectra were obtained by summing the  $Mn^{2+}(I)$ ,  $Mn^{2+}(II)$  and  $Mn^{2+}(III)$  spectra calculated with the SH parameters given in table 1.

We have obtained accurate SH parameter values for the  $Mn^{2+}$  centres in the cZnS:Mn QDs (table 1) by fitting both low and high frequency experimental EPR spectra with line shape simulations which included the forbidden transitions and line broadening effects, both strongly influenced by the non-cubic ZFS terms [16]. The increased accuracy also resulted from the narrower lines exhibited by the EPR spectra of the  $Mn^{2+}(I)$  centre (0.4 mT linewidth in the X-band, as compared to the best reported value of 0.6 mT [7]). The procedure for determining the SH parameters consisted of two steps. In the first step the  $g$  and  $A$  parameters were determined with high accuracy from fitting the line positions in the Q-band spectrum with transition fields calculated with a SH consisting of only the first two terms of Eq. (1). At such high magnetic fields the contributions of the ZFS terms to the line positions were found to be negligible (within the experimental errors). An accurate value for the  $D$  parameter was further determined from fitting the line shape of the more sensitive X-band spectrum. One should mention that in the case of a local axial crystal field, the cubic fourth order ZFS term characterized by the parameter  $a$  should be in principle replaced by an axial fourth order term characterized by the  $a-F$  parameter [3]. However, because of the small values of the fourth order ZFS terms, the strong line broadening effects, which were included as fluctuations in the ZFS parameter values to fit both X- and Q-band spectrum line shapes, are practically wiping out their contribution, making it impossible to determine their accurate values. Therefore, in our calculations we took the cZnS single crystal value  $a = 7.987 \times 10^{-4} \text{ cm}^{-1}$  [11]. The quality of the fitting with the experimental spectra (see figure. 1) demonstrates that the substitutional  $Mn^{2+}(I)$  EPR spectra lines are well described by the above mentioned SH, which includes, besides the isotropic terms with  $g$  and  $A$  values very close to those found in the cZnS single crystals, the axial ZFS term with  $|D| = 41 \times 10^{-4} \text{ cm}^{-1}$ . The resulting SH parameters presented in table 1 are also in excellent agreement with previously reported values we obtained by the analysis of the X (9.8 GHz) - and W (95 GHz)-band EPR spectra of the cZnS:Mn QDs [16].

As discussed in a separate article submitted for publication, the two surface  $\text{Mn}^{2+}$ (II) and  $\text{Mn}^{2+}$ (III) centres consist of  $\text{Mn}^{2+}$  ions localised at the surface of the cZnS:Mn NCs in partly oxidized areas, without or with an adsorbed water molecule attached, respectively.

**Table 1.** The SH parameters at RT for substitutional  $\text{Mn}^{2+}$  ions in cZnS:Mn QDs and single crystals, as well as of the surface  $\text{Mn}^{2+}$ (II) and  $\text{Mn}^{2+}$ (III) centres, determined in the present research. The hyperfine  $A$  and ZFS parameters  $a$ ,  $a-F$ ,  $D$  and  $E$  are given in  $10^{-4} \text{ cm}^{-1}$  units.

Lattice host/ $\text{Mn}^{2+}$ centre	Ref.	$g$	$A$	$ D $	$a$
<b>Mesop. cZnS:Mn NCs / <math>\text{Mn}^{2+}</math>(I)</b>	[This work ]	2.0022	-63.7	41	7.987 *
<b>Mesop. cZnS:Mn NCs / surface <math>\text{Mn}^{2+}</math>(II)</b>	[This work]	2.0012	-80.5	~10 -80	7.987 *
<b>Mesop. cZnS:Mn NCs / surface <math>\text{Mn}^{2+}</math>(III)</b>	[This work]	2.0009	-86.8	~ 10-80	7.987 *
<b>cZnS:Mn NCs/ NC1</b>	[5]	2.003	-64.5		
<b>cZnS:Mn NCs / SI</b>	[6]	2.0010	-63.9	1.0	
<b>ZnS:Mn NCs/ centre I</b>	[7, 8]	2.0024	-64.5	91.0	
<b>cZnS:Mn NCs /samples 1 and 2</b>	[9]	$g_{xx} = 2.0064$ $g_{yy} = 2.0064$ $g_{zz} = 2.0066$	$A_{xx} = -63.9$ $A_{yy} = -64.0$ $A_{zz} = -64.4$	37.4 $ E  = 12.47$	
<b>cZnS:Mn NCs / Ib</b>	[10]	$g_{\perp} = 2.0075$ $g_{\parallel} = 2.0040$	$A_{\perp} = -63.8$ $A_{\parallel} = -65.2$	37.4 $ E  = 12.47$	
<b>cZnS:Mn single crystal / substitutional <math>\text{Mn}^{2+}</math></b>	[11]	2.00225	-63.88	0	7.987
<b>Mixed polytype ZnS:Mn single crystal / trig. <math>\text{Mn}^{2+}</math> (PN centre)</b>	[18,19]	2.0018	-64.9	36.1	7.35 $a-F = 7.4$
<b>Microtwined cZnS:Mn single crystal / trig. <math>\text{Mn}^{2+}</math> (PN centre)</b>	[20]	2.0016	-64.5	37.85	$a-F = - 7.5$

\* Ref. [11]

The additional non-cubic ZFS term involved in describing the EPR spectrum of the substitutional  $\text{Mn}^{2+}$  ions in our investigated cZnS:Mn QDs is related with the presence of a local axial crystal field component (or local distortion of the lattice) at the cation  $\text{Zn}^{2+}$  site, with otherwise cubic ( $T_d$ ) symmetry in the bulk cZnS single crystals [11]. The resulting value of the  $D$  parameter suggests a unique configuration with a neighbouring defect, either as an unintentional impurity, or as an intrinsic lattice defect. A neighbouring impurity seems unlikely, because the estimated ~200 ppm concentration of  $\text{Mn}^{2+}$  ions in our cZnS:Mn QDs is too high compared to the trace impurity levels in the starting materials. A neighbouring intrinsic point defect (vacancy/interstitial) is also unlikely, in view of the similar electrical charges and close radii of the  $\text{Mn}^{2+}$  impurity and substituted  $\text{Zn}^{2+}$  cation. Also, a local axial crystal field resulting in a ZFS term with finite  $D$  parameter value could not be caused by the presence of size induced strains in the QDs [17]. The random character of such strains can only contribute to the experimentally observed inhomogeneous broadening of the EPR lines in QDs. Another more likely explanation results from comparing the SH parameters of the substitutional  $\text{Mn}^{2+}$  (I) centre with the corresponding parameters of the substitutional  $\text{Mn}^{2+}$  (PN) centre with trigonal symmetry reported in mixed polytype ZnS or microtwined cZnS single crystals [18-20], which exhibits a comparable  $D$ -value. It has been shown from correlated theoretical calculations and optical investigations that the trigonal PN centres consist of substitutional  $\text{Mn}^{2+}$  ions at  $\text{Zn}^{2+}$  sites where the normal stacking sequence of layers along the sphalerite  $\langle 111 \rangle$  direction (equivalent to the  $c$ -axis in wurtzite), at the third order neighbouring ligands, was changed by the gliding of a neighbouring layer due to a stacking fault or twin. From the close values of the axial ZFS parameter  $D$  of the PN centre in ZnS:Mn single crystals and the  $\text{Mn}^{2+}$  (I) centre in the cZnS QDs one concludes that in the later case the substitutional  $\text{Mn}^{2+}$  impurity is localized in a  $\{111\}$  layer, which contains the  $\text{Mn}^{2+}$  ion and its

tetrahedrally coordinating sulphur ligands, lying next to a stacking fault or twin. The resulting PN centre-type configuration, illustrated in figure 2 in comparison with an unperturbed substitutional localization in the  $cZnS$  lattice, is characterized by a local axial (trigonal) crystal field at the substitutional  $Mn^{2+}$  impurity ion and the additional axial ZFS term in the SH. The small differences in the SH parameters of the substitutional  $Mn^{2+}(I)$  centres in the  $cZnS$  QDs and of the PN centre in the defective  $ZnS$  single crystals (see table 1) are very likely due to experimental errors and/or slight differences in the arrangement of the first neighbouring ligands for the crystals and nanocrystals, respectively.

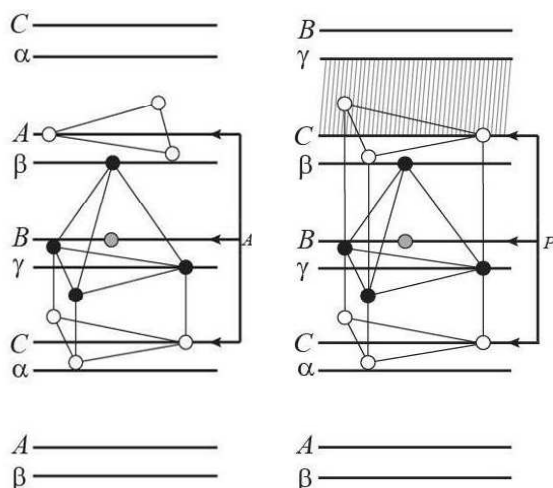


**Figure 2.** The local structure at the substitutional  $Mn^{2+}$  ions, shown in the left hand drawing for a pure cubic  $ZnS$  single crystal lattice and in the right hand drawing for a  $ZnS$  crystal lattice perturbed by the presence of a neighbouring stacking fault (shaded area) resulting in a trigonal distortion at the  $Mn^{2+}$  ion (grey), called the PN centre. In both drawings the  $Zn^{2+}$  cations and  $S^-$  anions are represented by open and filled circles, respectively, aligned as  $\{111\}$  layers.

In order to confirm the validity of the proposed neighbouring extended lattice defect (ELD) model for the localization of the  $Mn^{2+}$  ions in the  $cZnS:Mn$  QDs we had to prove that a rather large concentration of such defects exists in the investigated samples. In crystals with a sphalerite structure, planar stacking defects such as stacking faults and twins are known to occur along the  $\{111\}$  planes. To reveal the stacking defects in the cubic  $ZnS:Mn$  nanoparticles high resolution transmission electron microscopy (HRTEM) investigations were performed.

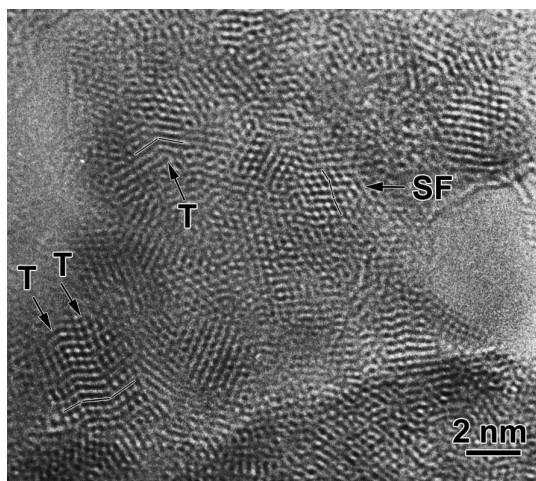


**Figure 3.** HRTEM image of a mesoporous  $cZnS:Mn$  sample, previously investigated by EPR spectroscopy, revealing in some crystallites (marked by arrows) planar defects such as twin interfaces (T) and stacking faults (SF).

The atomic structure of the extended defects can be imaged by HRTEM only if the defects exhibit translation symmetry along the viewing direction. For crystals with a sphalerite structure this condition is fulfilled along the  $[110]$  viewing direction. Figure 3 shows a HRTEM image of a very thin part of a

cZnS:Mn sample which has been previously investigated by EPR spectroscopy. As shown in the picture some of the ZnS nanocrystals exhibit defects such as twins (T) or stacking faults (SF), marked by arrows. Any substitutional impurity localized next to these atomic planes will be therefore in a disturbed neighbourhood, with regard to the perfect cubic lattice.

By examining several HRTEM images we found out that a large amount (at least 30%) of the ZnS:Mn nanocrystallites oriented along [110] contain planar extended defects in the form of stacking faults and twins. Considering that the ZnS:Mn nanocrystallites are arbitrarily oriented in the investigated sample, it results that a corresponding fraction of all nanocrystallites contain such extended defects. The observation of the extended defects by HRTEM also confirms the simulation results based on a Debye function analysis, which has shown [21] that the presence in small cZnS:Mn nanocrystals of extended defects in the form of twins is essential for an accurate fitting of the experimental XRD patterns.

#### 4. Conclusions

Considering that no sizable amount of substitutional  $Mn^{2+}$  ions localized at unperturbed  $Zn^{2+}$  with  $T_d$  symmetry could be identified in our investigated mesoporous cZnS:Mn, it results that the ELDs in the form of stacking faults and twins are essential in the localization of the  $Mn^{2+}$  ions in the cZnS QDs.

The presence of a local axial ZFS term of comparable magnitude in the SH describing the EPR spectrum of substitutional  $Mn^{2+}$  ions has been also reported in cubic CdS nanocrystals [22] and occurs very likely in ZnSe:Mn nanocrystals, which also exhibit forbidden hyperfine transitions in the  $Mn^{2+}$  EPR spectrum [23]. Therefore, it is reasonable to assume that a similar structure involving a neighbouring extended defect is valid for the substitutional  $Mn^{2+}$  ions in other cubic II-VI semiconducting nanocrystals.

The localization of the substitutional  $Mn^{2+}$  in the II-VI semiconductor QDs next to ELDs has some important implications. It demonstrates that the ELDs play an essential role in the incorporation of  $Mn^{2+}$  and possibly of other divalent impurities in the very small nanocrystals (QDs), which usually do not exhibit well defined facets, essential for the diffusion assisted incorporation of impurities [2]. On the other hand, it is well known that defects such as steps on the surfaces or dislocations, which emerge when the extended defects intersect the nanocrystals surface, are very likely to "attract" impurities [24]. Therefore, one expects the doping to be controlled mainly by the trapping of impurities at the steps and dislocations at the surface of the growing nanocrystals.

The large fraction of planar extended defects observed in our investigated cZnS:Mn QDs samples can explain the relatively high fraction of the doping  $Mn^{2+}$  impurities (more than 10%) contained in our samples, including the formation of impurity aggregated states at higher dopant concentrations, previously reported in ZnS nanocrystals of comparable size [6-8,10]. Moreover, according to our results, at higher dopant concentrations one expects the impurities to aggregate preferentially in {111} planes parallel to the extended defects, resulting in specific properties which should be further investigated.

In summary, we conclude that the high doping levels of  $Mn^{2+}$  ions in the cubic II-VI semiconductor QDs prepared by colloidal growth are very likely controlled by the mechanism of extended lattice defects assisted incorporation of impurities. This mechanism also explains the reported localization of  $Mn^{2+}$  impurities at cation sites situated next to an extended lattice planar defect, resulting in a local crystal lattice deformation at the impurity ion, which should be also taken into consideration in the description of the local quantum states and resulting optical, electrical and magnetic properties.

#### Acknowledgements

The financial support by CNCSIS-UEFISCSU under project number PN-II-ID-523/2008 is gratefully acknowledged.

#### References

- [1] Erwin S C, Zu L, Haftel M I, Efros A L, Kennedy T A and Norris D J 2005 *Nature* **436** 91- 94

- [2] Norris D J, Efros A L and Erwin S C 2008 *Science* **319** 1776 -79
- [3] Abragam A and Bleaney B **1970** Electron Paramagnetic Resonance of Transition Ions, Clarendon Press, Oxford
- [4] Hu H and Zhang W **2006** *Opt. Mat.* **28** 536-50.
- [5] Kennedy T A, Glaser E R, Klein P B and Bhargava R N, **1995** *Phys.Rev. B* **52** R14356-59
- [6] Borse P H, Srinivasa D, Shinde R F, Date S K, Vogel W and Kulkarni S K **1999** *Phys. Rev. B* **60** 8659- 64
- [7] Igarashi T, Ihara M, Kusunoi T, Ohno K, Isobe T and Senna M **2001** *J. Nanoparticles Res.* **3** 51-56
- [8] Igarashi T, Isobe T and Senna M 1997 *Phys. Rev. B* **56** 6444-45
- [9] Gonzalez Beermann P A, McGarvey B R, Muralidharan S and Sung R C W **2004** *Chem. Mater.* **16** 915-18
- [10] Gonzalez Beermann P A, McGarvey B R, Skadtchenko B O, Muralidharan S and Sung R C W, **2006** *J. Nanoparticles Res.* **8** 235-41
- [11] Nistor S V and Stefan M **2009** *J. Phys.: Condens. Matter* **21** 145408 (7pp)
- [12] Nistor L C, Mateescu C D, Birjega R and Nistor S V, **2008** *Appl. Phys. A* **92** 295-301
- [13] Nistor S V, Nistor L C, Stefan M, Mateescu C D, Birjega R, Solovieva N and Nikl M **2009** *Superlatt. and Microstruct.* **46** 306-11
- [14] Nistor S V, Nistor L C, Stefan M, Ghica D, Mateescu C D and Birjega R **2010** *Rom. Repts. Phys.* **62** 319-328
- [15] Rubio J O, Munoz P E, Boldu O J, Chen Y and Abraham M. M **1979** *J. Chem. Phys.* **70** 633-38
- [16] Nistor S V, Stefan M, Nistor L C, Goovaerts E and Van Tendeloo G **2010** *Phys. Rev. B* **81** 035336 (6pp)
- [17] Qadri S B, Skelton E F, Hsu D, Dinsmore A D, Yang J, Gray H F and Ratna B R **1999** *Phys. Rev. B* **60** 9191-93
- [18] Lambert B, Buch T and Clerjaud B **1972** *Sol. State Commun.* **10** 25-27
- [19] Buch T, Clerjaud B, Lambert B and Kovacs P **1973** *Phys. Rev. B* **7** 184-91
- [20] Yakunin A Ya, Shtambar I V, Kushnir A S and Omelchenko S A **1973** *Russian Phys. J.* **16** 1375-79
- [21] Vogel W, Borse P H, Deshmuck N and Kulkarni S K **2000** *Langmuir* **16** 2032-37
- [22] Counio G, Esnouf S, Gascoin T and Boilot J -P **1996** *J. Phys. Chem.* **100**, 20021-26
- [23] Norman T J Jr., Magana D, Wilson T, Burns C, Zhang J Z, Cao D and Bridges F **2003** *J. Phys. Chem. B* **107**, 6309-17
- [24] Amelinckx S **1964** *The Direct Observation of Dislocations*. In *Solid State Physics: Advances in Research and Applications*. Suppl. 6; p 55-89, Seitz F. & Turnbull D., Eds., Academic Press: New York